Sustainable formation of tricarballylic acid from citric acid over highly stable $Pd/Nb_2O_5.nH_2O$ catalysts

Sustainable formation of tricarballylic acid from citric acid over highly stable Pd/$Nb_2O_5.nH_2O$ catalysts

*Wouter Stuyck[†], Aram L. Bugaev[‡], Tom Nelis[†], Rodrigo de Oliveira-Silva[†], Simon Smolders[†], Oleg A. Usoltsev[‡], Daniel Arenas Esteban[ⁱ], Sara Bals[ⁱ], Dimitrios Sakellariou[†], Dirk De Vos[†]**

[†]Centre for Membrane Separations, Adsorption, Catalysis and Spectroscopy for Sustainable Solutions (cMACS) , KU Leuven, 3001 Leuven, Belgium

[‡]The Smart Materials Research Institute, Southern Federal University, Sladkova 178/24, 344090 Rostov-on-Don, Russia.

[ⁱ]EMAT, University of Antwerp, Groeneborgerlaan 171, 2020 Antwerp, Belgium.

*Corresponding author; email: dirk.devos@kuleuven.be

KEYWORDS

Heterogeneous catalysis, dehydration, hydrogenation, biomass, niobium oxides, palladium, bifunctional catalysts.

HIGHLIGHTS

- $Nb_2O_5.nH_2O$ proved to be a stable and efficient catalyst for the dehydration of citric acid at mild reaction temperatures
- Investigation of the interaction of citric acid with the $Nb_2O_5.nH_2O$ surface by ^{13}C MAS NMR
- Synthesis of bifunctional $Pd/Nb_2O_5.nH_2O$ via a low-temperature reduction method to preserve the acid properties of the support
- Yields of tricarballylic acid exceeding 90% over multiple runs

ABSTRACT

Recently, a reaction sequence was developed for the production of tricarballylic acid, an interesting plasticiser precursor, from citric acid by using a H-Beta zeolite and Pd/C catalyst. Although yields of 85% of tricarballylic acid were obtained, citric acid elicited Al leaching from the zeolite framework, resulting in loss of activity. In this work, $Nb_2O_5.nH_2O$ was found to be a stable and performant catalyst for this reaction, and a strong involvement of the hydroxyl group of citric acid with the $Nb_2O_5.nH_2O$ surface was observed by ^{13}C MAS NMR. Next, $Pd/Nb_2O_5.nH_2O$ catalysts were synthesized via a low temperature reduction method to preserve the acidity of the $Nb_2O_5.nH_2O$ support; the nature of the Pd phase was examined by XAS. In presence of a 0.6 wt% $Pd/Nb_2O_5.nH_2O$ catalyst, yields over 90% of tricarballylic acid were obtained over multiple runs. Finally, this catalyst was also suitable for the dehydration-hydrogenation of other monohydroxy carboxylic acids.

1. INTRODUCTION

Increasing awareness of the bio-accumulating and endocrine disrupting properties of traditional ortho-phthalate plasticisers has led to serious restrictions on these compounds and a growing

interest in safe alternatives.[1,2] Numerous alternatives focus on developing structures that are similar but less toxic than ortho-phthalates, like terephthalates, trimellitates and cyclohexanoates.[2] However, with the tendency to explore renewable resources for the production of drop-in chemicals or novel compounds, the potential of biobased plasticisers as safe alternatives is more and more investigated.[3] Several renewable substrates and derived plasticisers have been defined so far,[3-8] of which those that are based on citric acid can be considered as one of the most appealing classes.[9] Citric acid is a widely abundant and thus cheap renewable resource since it is produced via a high yield fermentation process, resulting in an annual production volume of 2 million tons in 2016.[10] In addition, citric acid based plasticisers, such as acetyl tributyl citrate (ATBC) or butyryl trihexyl citrate (BTHC), possess comparable plasticising properties as the traditional bis(2-ethylhexyl) phthalate (DEHP) plasticiser.[9,11] Nevertheless, the acetylation or butyrylation of citrate esters to respectively ATBC and BTHC involves the use of anhydrides and strong homogeneous Brønsted acid catalysts,[12] resulting in stoichiometric waste and harsh acidic conditions. Furthermore, ATBC is known to be more prone to leaching from the plastic matrix compared to DEHP, making it a less efficient plasticiser.[9,13,14]

An alternative, but closely related class of plasticisers consists of tricarballylate esters. These plasticisers are in fact very similar to citrate plasticisers, with the only difference that the polar hydroxyl group of citric acid is absent rather than being derivatised via an acetylation or butyrylation. The resulting tricarballylate plasticisers possess excellent plasticizing efficiency in polyvinyl chloride (PVC) resins, including a brittle point, elongation at break, modulus at 100% and tensile strength comparable to or better than those obtained with DEHP.[15,16] In spite of this, an efficient route towards tricarballylic acid from the abundant citric acid was not described, until the development of a one-pot sequential dehydration-hydrogenation of citric acid to tricarballylic

acid.[17] The first step of this reaction is a dehydration of citric acid (**1** in Scheme 1) to aconitic acid (**2**), followed by a hydrogenation to tricarballylic acid (**3**). To avoid the spontaneous decarboxylation of aconitic acid (**2**) to itaconic acid (**4**) and obtain a high selectivity towards tricarballylic acid (**3**), the reaction temperature was kept mild. However, at lower temperatures, the dehydration of citric acid (**1**) to aconitic acid (**2**) became slow. Therefore, the dehydration reaction was enhanced by adding a solid acid zeolite catalyst in combination with a small amount of Pd/C to perform the subsequent hydrogenation. Especially low Si/Al H-Beta zeolites proved to be efficient as dehydration catalysts, which was attributed to the large pore dimensions of H-Beta zeolites and to the combined action of Lewis and Brønsted acid sites in the zeolite channels. Under relatively mild reaction conditions (160 °C, 10 bar H_2), a yield of 85% of tricarballylic acid was achieved by reacting citric acid in water for 20 h in presence of 0.5 mol% Pd/C and 5 wt% H-Beta zeolite. However, due to the corrosive nature of citric acid, the framework aluminum of the zeolite material was partially leached out, leading to a loss of acid sites and a decreased activity of the H-Beta catalyst upon recycling.[17]

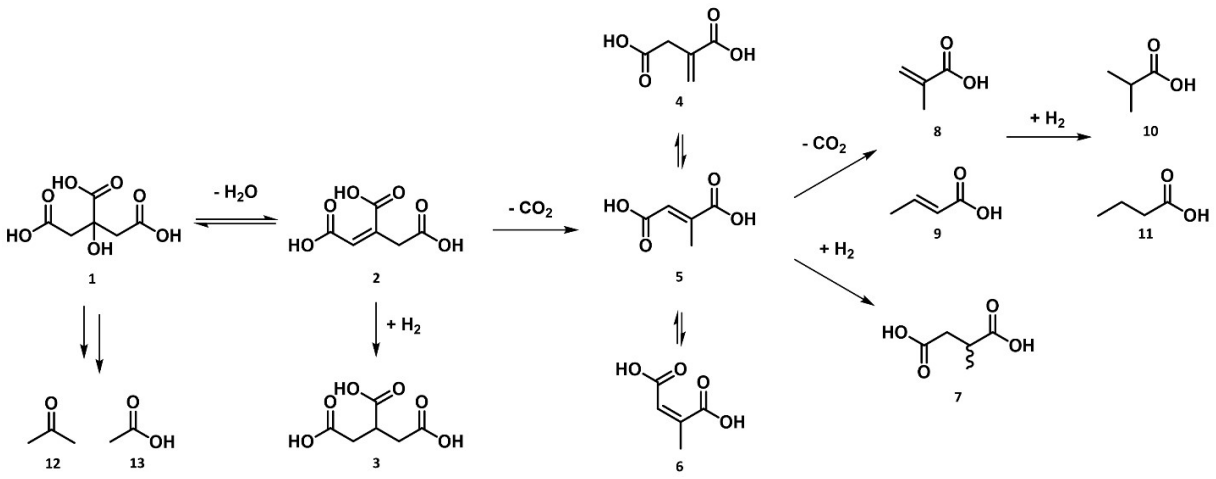

Scheme 1. Reaction scheme of the dehydration-hydrogenation of citric acid with undesirable side reactions

This prompted us to search for solid acid catalysts that would be active for the dehydration of citric acid and would be able to withstand the corrosive aqueous citric acid conditions. In this respect, niobium oxides are known to be stable in acidic aqueous media [18,19] and to possess efficient dehydration activity under aqueous conditions.[18,20-24] For example the dehydration-isomerisation of dihydroxyacetone to lactic acid [18] and the hydrogenation-cyclization of levulinic acid to γ-valerolactone[19] are reported to be efficiently catalysed by niobium oxides, whereby these materials remained active and stable under the applied reaction conditions. In this work, the potential of niobium oxide materials for the sequential dehydration-hydrogenation reaction of citric acid to tricarballylic acid (Scheme 2) has been investigated. Two scenarios are envisaged: (i) a two-catalyst one-pot system of niobium oxide together with Pd/C, and (ii) a system containing Nb_2O_5 as a solid acid support to form bifunctional $Pd/Nb_2O_5.nH_2O$ materials.

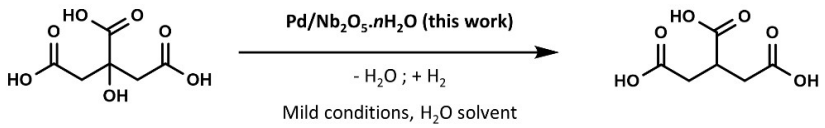

Scheme 2. Sequential dehydration-hydrogenation of citric acid.

2. RESULTS AND DISCUSSION

2.1. Nb_2O_5 oxides as solid acids in a two-catalyst one-pot system

Previous research on the sequential dehydration-hydrogenation of citric acid (**1**) to tricarballylic acid (propane-1,2,3-tricarboxylic acid; PTA) (**3**) in the presence of H-Beta zeolites, pointed out that especially a large number of Brønsted acid sites in combination with Lewis acidity resulted in an efficient dehydration of citric acid (**1**) to aconitic acid (**2**). The subsequent hydrogenation of aconitic acid (**2**) to PTA (**3**) seemed to be less challenging in comparison to the preceding dehydration reaction, while the undesired decarboxylation of aconitic acid (**2**) to itaconic acid (**4**)

was predominantly temperature controlled (reaction network in Scheme 1).[17,25-27] In the search for stable solid acid dehydration catalysts, two Nb_2O_5 materials were selected and synthesized; they both possess a significant amount of both Brønsted and Lewis acid sites (Table 2). Moreover, the acidity of both $Nb_2O_5.nH_2O$ and ortho-Nb_2O_5 is reported to remain effective in aqueous media, while the materials themselves are reported to be highly durable.[18,24,28] In an initial catalyst screening, two self-synthesized catalysts, as well as commercial Nb_2O_5 and $Nb_2O_5.nH_2O$ were compared to the previously reported zeolite system in a two-catalyst one-pot system with a small amount of Pd/C (Table 1).

Table 1. Sequential dehydration-hydrogenation of citric acid. [a]

				Substrate [%][c]			Selectivity [%]			
	Acid Catalyst	Pd/C[b] [mol%]	T [°C]	Citric acid	Citrate[d]	X [%][e]	PTA[f]	MSA[g]	Fragmentation[h]	Mole balance [%]
1	-	0.5	150	92	0	8	88	8	4	> 99
2	Nb_2O_5 [i]	0.5	150	91	0	9	72	6	22	98
3	*Ortho*-Nb_2O_5	0.5	150	46	0	41	84	15	1	87
4	$Nb_2O_5.nH_2O$ [i]	0.5	150	52	0	44	91	8	1	96
5	$Nb_2O_5.nH_2O$	0.5	150	17 (39)[j]	0	56	95	2	3	73 (95)[j]
6[k]	$Nb_2O_5.nH_2O$	0.5	150	28	0	64	87	12	1	92
7	$Nb_2O_5.nH_2O$	1.0	150	8	0	73	95	4	1	81
8	$Nb_2O_5.nH_2O$	0.5	160	< 1	0	85	91	9	< 1	85
9	$Nb_2O_5.nH_2O$	1.0	160	< 1	0	86	91	8	1	86
10	H-Beta 10.8[l]	0.5	150	3	18	80	96	3	< 1	> 99
11	H-Beta 10.8[l]	0.5	160	< 1	5	95	90	9	< 1	> 99

[a] Reaction conditions: Citric acid (0.2 mmol) in water (2 mL), 0.1 g of acid catalyst, 10 bar H_2, 20 h. [b] mol% of Pd (5 wt% Pd/C) with respect to citric acid. [c] Remaining amount of substrate, as a percentage of the initial amount of substrate, that is detected in the reaction mixture without performing desorption of the strongly adsorbed species on the catalytic surface. [d] The amount of citric acid that is present as citrate salt determined by ^{1}H-NMR after acidifying the mixture (See ESI). [e] Conversion: sum of the amount of detected products in the reaction mixture divided by the initial amount of citric acid that was added. Potentially adsorbed species are not taken into account; these consist solely of citric acid (See entry 5 with superscript [j] and ESI). [f] Propane-1,2,3-tricarboxylic acid. [g] Methylsuccinic acid. [h] 'Fragmentation' represents the fragmented products acetone and acetic acid. [i] Commercial catalyst. [j] Mole balance and distribution of citric acid, with numbers between brackets include the amount of citric acid after desorption from the $Nb_2O_5.nH_2O$ after reaction (See ESI). [k] Entry 6 shows the recycling experiment of entry 5, where the catalytic system is directly recycled after two washing steps with water (See ESI). [l] Si/Al ratio of 10.8.

The commercial Nb_2O_5 (entry 2) was ineffective to catalyze the dehydration of citric acid (**1**) since no significant improvement was noticed for the citric acid conversion compared to the reaction without an acid catalyst (entry 1). Both the *ortho*-Nb_2O_5 and $Nb_2O_5.nH_2O$ materials show a clear increase in conversion of citric acid, while for both $Nb_2O_5.nH_2O$ catalysts also a high selectivity towards PTA is observed (entry 3, 4 and 5). The difference in the activity of the Nb_2O_5 catalysts can be explained by their differences in acid site densities; based on the data shown in Table 2, the self-synthesized $Nb_2O_5.nH_2O$ possesses a higher density of Brønsted and Lewis acid sites compared to *ortho*-Nb_2O_5 and a higher density of Brønsted acid sites compared to the commercial $Nb_2O_5.nH_2O$. While fewer Lewis acid sites are present on *ortho*-Nb_2O_5 than on $Nb_2O_5.nH_2O$, the Lewis acid sites of *ortho*-Nb_2O_5 are known to be more stable in the presence of water.[18] From the data, it can also be concluded that Brønsted acid sites are important for the dehydration of citric acid (Table 1, entries 4 and 5): the sample with a larger number of Brønsted acid sites, viz. the self-synthesized $Nb_2O_5.nH_2O$, gives a faster conversion than the commercial $Nb_2O_5.nH_2O$, with a smaller number of Brønsted acid sites.

Table 2. Acid site densities of Nb_2O_5 solid acid catalysts estimated by pyridine-adsorption measurements with FTIR.

	Acid site density (μmol/g)	
Catalyst	Brønsted acid	Lewis acid
Ortho-Nb_2O_5	124	179
$Nb_2O_5.nH_2O$ (commercial)	123	253
$Nb_2O_5.nH_2O$ (self-synthesized)	206	251

Further optimization of the reaction conditions was performed with the self-synthesized $Nb_2O_5.nH_2O$ as the solid acid, and included an increase of the amount of Pd/C to 1 mol% (entry 7), an increase of the reaction temperature (entry 8) and a combination of both (entry 9). Increasing the amount of Pd/C at a reaction temperature of 150 °C resulted in both an increase of the citric

acid (**1**) conversion and the selectivity towards the desired product PTA (**3**) (entry 7). The larger amount of Pd/C in the reaction mixture increases the hydrogenation rate of the dehydrated intermediate aconitic acid (**2**) to PTA (**3**). Increasing the reaction temperature resulted in a significant effect on the citric acid conversion (**1**), reaching 85% at 160 °C (entry 8). Also a marked increase in selectivity for MSA (**7**) is noticed at higher temperatures, indicating that a higher temperature not only enhances the dehydration of citric acid (**1**) to aconitic acid (**2**) but also the decarboxylation of aconitic acid (**2**) to itaconic acid (**4**). Increasing the amount of Pd/C at this elevated temperature did not further improve the conversion of citric acid (**1**) nor the selectivity to PTA (**3**) (entry 9).

When the activity of $Nb_2O_5.nH_2O$ (entry 5 & 8) is compared to that of H-Beta (entry 10 & 11), it is seen that the low Si/Al H-Beta zeolite is more active, since the respective citric acid conversions are higher at both reaction temperatures. However, regarding selectivity towards the desired PTA (**3**) product, both catalytic systems seem to perform equally well. Comparing product mixtures formed with both catalysts, no new dissolved or volatile side products were produced in the case of $Nb_2O_5.nH_2O$, and the NMR data show no formation of citrate species in the reaction mixture (ESI, Figure S1). This is in sharp contrast to previous research, where the presence of a significant fraction of Al-citrate indicated dealumination of the H-Beta zeolite under reaction conditions.[17] The stability of the Nb_2O_5 materials was subsequently confirmed by performing Nb-ICP on the crude reaction mixtures; the amount of Nb remained below the detection limit of 50 ppb (0.0005% of the total amount of catalyst). However, in presence of Nb_2O_5 solid acids, and especially in presence of the self-synthesized $Nb_2O_5.nH_2O$, an incomplete mole balance was observed. This might indicate that some reaction products are not taken into account, though no new species were detected in the ^{1}H-NMR spectra of the crude reaction mixtures. Another option is that some species

are strongly adsorbed on the oxophilic $Nb_2O_5.nH_2O$ catalyst, leading to a decreased concentration of organic molecules in the reaction mixture. To elucidate this mole balance deficiency, several efforts were made. First, a desorption experiment with 37 wt% DCl in D_2O was performed on the isolated and dried catalysts of entry 5 (See ESI, 2.1). From this experiment, it was concluded that an additional 22% of citric acid was still adsorbed on the $Nb_2O_5.nH_2O$, which covers almost completely the initial deficiency in mole balance (entry 5 between brackets). Interestingly, only citric acid was observed after desorption, indicating a strong preferential interaction of the citric acid with the $Nb_2O_5.nH_2O$ surface. Next, (competitive) adsorption experiments were conducted from which it could be concluded that citric acid preferentially adsorbs on the $Nb_2O_5.nH_2O$ surface, even if it is present in a minor fraction compared to MSA and PTA (Table S1). This preferential interaction of $Nb_2O_5.nH_2O$ with citric acid as the substrate compared to the saturated products, also ensures that newly formed product molecules are effectively desorbed and replaced by new substrate molecules. Finally, when both catalysts (Pd/C & $Nb_2O_5.nH_2O$) are directly reused in a new catalytic cycle (See ESI, 1.7), the mole balance increases significantly (entry 6), indicating that the surface of $Nb_2O_5.nH_2O$ became saturated with citric acid (**1**) during the first cycle. Noteworthily, the strong adsorption of citric acid (**1**) does not hamper the activity of the $Nb_2O_5.nH_2O$ since a clear increase in conversion of citric acid (**1**) to 64% was observed. This confirms that $Nb_2O_5.nH_2O$ can withstand the acidic aqueous conditions and is a stable and efficient solid acid catalyst. However, a noticeable drop in the selectivity towards PTA (**3**) is observed as well.

When the sequential dehydration-hydrogenation of citric acid is evaluated over time (Figure 1, Profile A), an almost linear increase of PTA (**3**) and linear decrease of citric acid (**1**) are observed; only a very small amount of side product is formed, which mainly consists of MSA (**7**). After 2 h,

a deficiency in mole balance is observed, after which the mole balance remains more or less constant. Although it was elucidated that this deficiency originates from strong citric acid adsorption on $Nb_2O_5.nH_2O$ (*vide supra*), it remains difficult to make any firm conclusions on the reactivity and kinetics of the catalytic system with an incomplete mole balance. Therefore, a protocol was developed to presaturate the $Nb_2O_5.nH_2O$ surface with citric acid (see ESI 2.3), after which this presaturated $Nb_2O_5.nH_2O$ was applied for kinetic experiments under different selected reaction conditions (Figure 1 & Table S2, Profiles B-F). High mole balances (95% - 100%) were obtained in almost all cases. Applying a presaturated catalyst under standard reaction conditions resulted in similar trends as with a bare $Nb_2O_5.nH_2O$, but slightly higher yields of PTA and MSA were obtained. This aligns with the recycling experiment of Table 1 (entry 6), where an increase in conversion and small decrease in selectivity to PTA were observed. By varying the amounts of either catalyst (Profile B vs. C and D), it can be concluded that the dehydration is the slower step in the sequential process, since a five-fold decrease of $Nb_2O_5.nH_2O$ reduced the conversion of citric acid substantially, while a five-fold decrease of the amount of Pd had only a minor effect on the PTA yield after 20 h. As expected, some increase in side product formation (especially MSA) was observed when the hydrogenation capacity of the system was decreased (Profile D). Interestingly, decreasing the H_2 pressure to 2 bar did not have a major effect on the PTA yield (Profile E). Applying the presaturated $Nb_2O_5.nH_2O$ under optimized conditions of Table 1 (entry 9; 160 °C, 1 mol% Pd), did result in a significantly faster conversion of citric acid (Profile F). However, a large fraction of the dehydrated aconitic acid followed the undesired decarboxylation route, since up to 24% MSA was detected in the reaction mixture. Overall, the analysis of the kinetic experiments strongly supports the reaction network as proposed in Scheme 1.

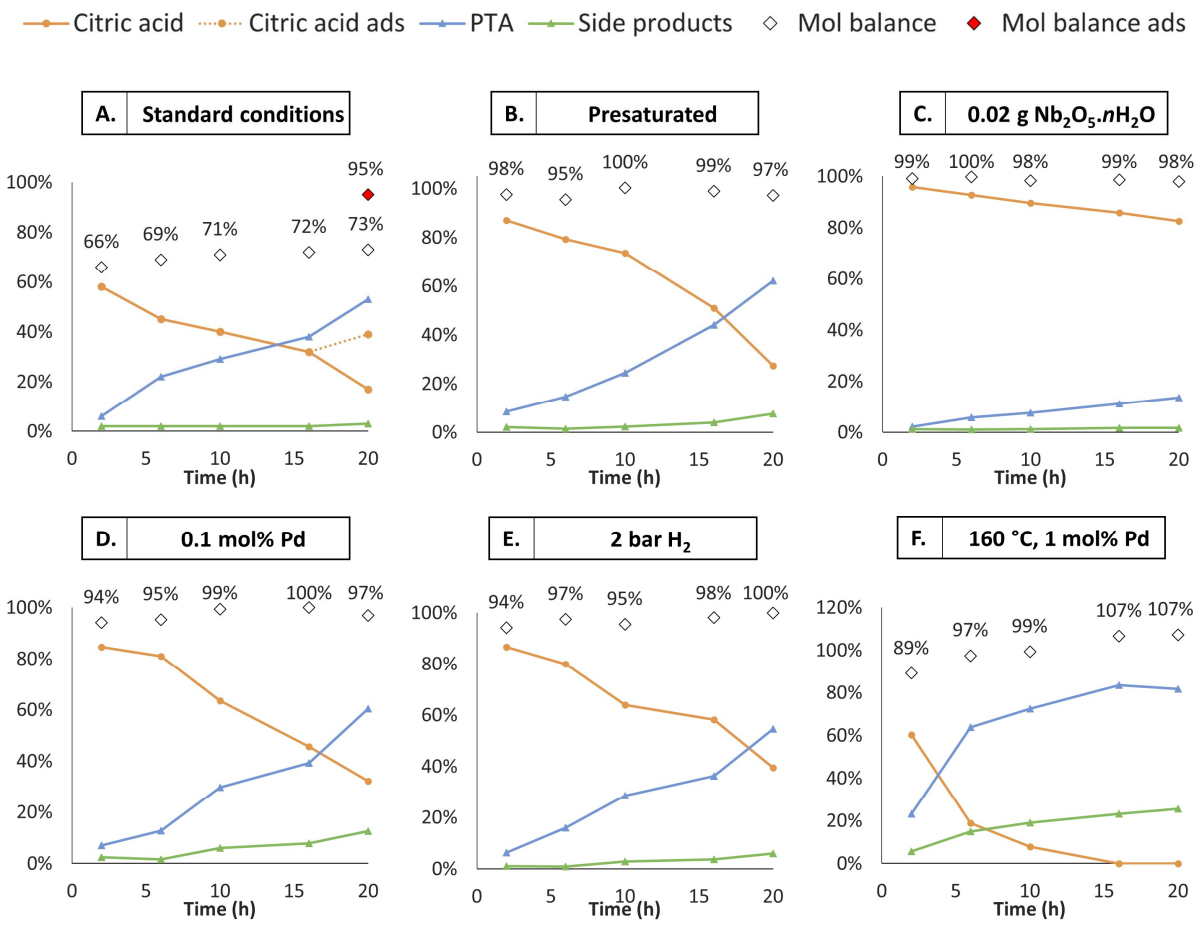

Figure 1. Time profiles of the sequential dehydration-hydrogenation of citric acid under different reaction conditions. Each set of data points at a specific time corresponds to a different batch reaction. Profile A: Standard reaction conditions: citric acid (0.2 mmol), water (2 mL), 0.1 g $Nb_2O_5.nH_2O$, 0.5 mol% Pd (5 wt% Pd/C), 150 °C, 10 bar H_2. Profile B - F: performed with 0.1134 g presaturated $Nb_2O_5.nH_2O$ catalyst (see ESI), with the deviation from the standard reaction conditions noted on top of the graph. Legend: citric acid (orange, full), citric acid corrected after desorption (orange, dashed), PTA (blue), side products* (green), mole balance (white diamond), mole balance corrected after desorption experiment (red diamond). * Side products consist of mainly MSA and maximum 2% of fragmented products in all cases. The mole balance exceeds 100% in profile F, indicating that some citric acid carried over from the presaturation is eventually converted.

2.2. Interaction of citric acid with $Nb_2O_5.nH_2O$

From the previous results and the desorption experiment, it is clear that citric acid strongly interacts with the $Nb_2O_5.nH_2O$ surface. In fact, it adsorbs highly preferentially in presence of other saturated

organic acids like PTA and MSA, even when its initial concentration is lower than that of PTA in the reaction mixture (See ESI, Table S1). Studies on the complexation of citric acid and PTA with homogeneous Al^{3+} state that Al citrate is a 270 times more stable complex compared to Al 3-carboxy-1,5-pentanedioate because of the involvement of the tertiary hydroxyl group in the chelation of citric acid with Al.[29] For a solid surface, the adsorption of both compounds can strongly depend on the nature of the heterogeneous solid, as well as on the pH of the reaction mixture. Under aqueous acidic conditions, like in the reaction mixtures of this work, the consensus in literature seems to be that citric acid mainly adsorbs via its carboxylic acid groups on oxide surfaces, leaving the hydroxyl group untouched.[30-32] Hidber et al. suggest that the hydroxyl group is involved in the binding of citric acid on an alumina surface. However, unambiguous evidence for such an interaction was not provided in their work.[33]

To investigate the coordination of citric acid on oxide materials, attenuated total reflection-Fourier transform infrared (ATR-FTIR) spectral deconvolution has been employed.[29-32] In this work however, considering the significant amount of citric acid that is adsorbed on $Nb_2O_5.nH_2O$, solid-state ^{13}C MAS NMR analysis was applied. Upon isolation of the $Nb_2O_5.nH_2O$ catalyst after a catalytic reaction, the recovered oxide is measured *via* 1D ^{13}C MAS NMR and the spectrum is compared with that of pure citric acid (Figure 2). By comparing the isotropic chemical shifts of citric acid for both cases, one clear difference can be observed: the carbon atom that is attached to the hydroxyl group of citric acid is shifted from 72 ppm to 85 ppm when citric acid is adsorbed on $Nb_2O_5.nH_2O$, and only a second minor peak at 73 ppm subsists. All the other peaks display the same chemical shift in both spectra; however the widths of the peaks are obviously larger for the case where citric acid is adsorbed on $Nb_2O_5.nH_2O$. A similar isotropic shift (from 74 ppm to 88 ppm) for the C-OH carbon atom was observed in the homogeneous complexation of Am^{3+} with

citric acid at low pH values. In this study Tamain et al. concluded, also based on other characterization data, that citric acid at pH 1 is preferentially coordinated with Am^{3+} in a 1:1 complex with two deprotonated carboxylic acids (terminal and central) and the hydroxyl group.[34] The observed shift for the adsorbed citric acid in Figure 2 thus strongly suggests a similar involvement of the hydroxyl group in the complexation of citric acid with the $Nb_2O_5.nH_2O$ surface. The fact that citric acid coordinates in such a way on a solid catalyst under aqueous acidic conditions can be considered as very remarkable, considering the strongly acidic and stringent environment surrounding the tertiary hydroxyl group of citric acid. This is also the first time that the involvement of the hydroxyl group in the complexation of citric acid on a heterogeneous surface is observed as clearly.

This strong interaction between a Lewis acid Nb cation and the hydroxyl group of citric acid likely activates the C-O bond of the hydroxyl group and therefore makes the adsorbed citrate molecule more prone to dehydration when it encounters a strong Brønsted acid site in its close vicinity. Since $Nb_2O_5.nH_2O$ possesses a significant amount of strong Brønsted acid sites (Table 2), this interaction with a Brønsted acid site is highly likely to occur on the $Nb_2O_5.nH_2O$ surface (Figure 3).

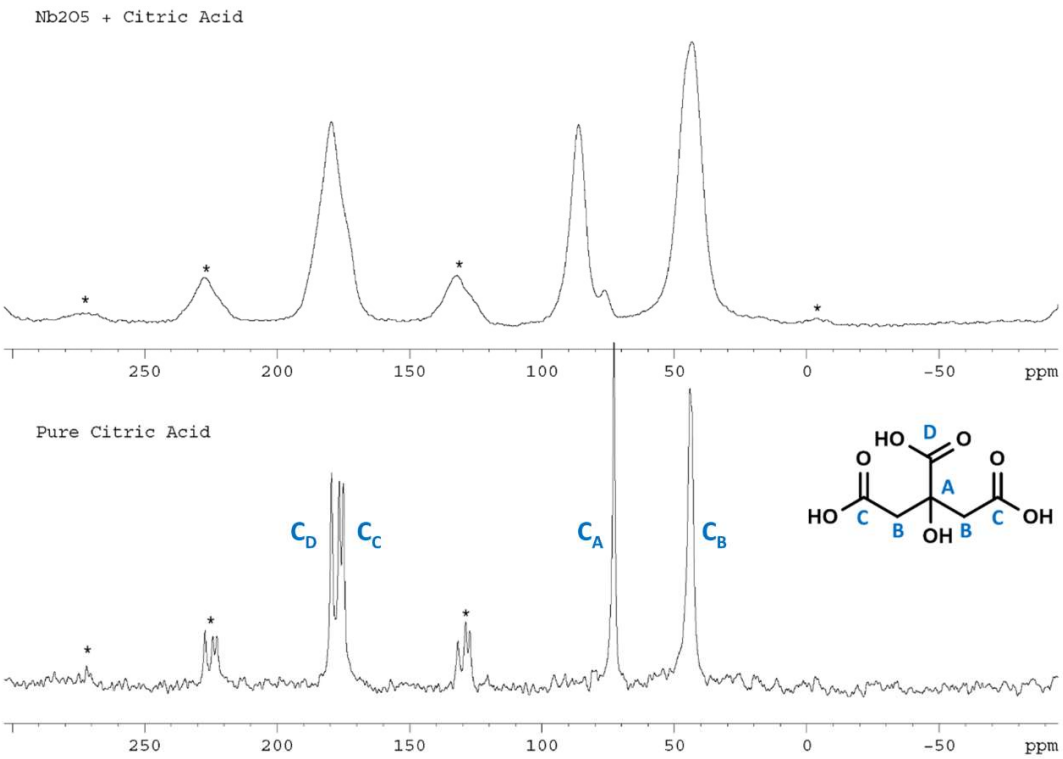

Figure 2. 1D ^{13}C MAS NMR spectra of pure citric acid (bottom) and citric acid adsorbed on the $Nb_2O_5.nH_2O$ catalyst (top). The peaks labeled with * are spinning side bands and can be neglected.

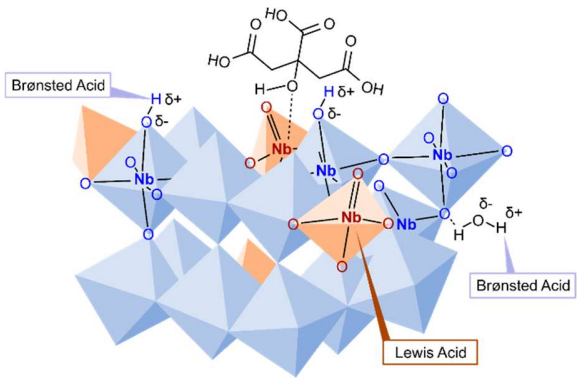

Figure 3. Schematic representation of the interaction of citric acid with the $Nb_2O_5.nH_2O$ surface.

2.3. Bifunctional Pd/$Nb_2O_5.nH_2O$ catalysts – Synthesis & Characterization

The promising results with the two-catalyst one-pot system, combined with the indication that $Nb_2O_5.nH_2O$ remains active and stable under the reaction conditions, prompted investigation of the possibility of synthesizing a bifunctional Pd/$Nb_2O_5.nH_2O$ catalyst. Immobilization of the Pd^0

nanoparticles on the $Nb_2O_5.nH_2O$ solid acid support would simplify the system and subsequent reuse of the catalyst, since there is only one solid in the reaction mixture. In addition, by minimizing the diffusion distance between the acid and metal sites, the intermediate aconitic acid can be hydrogenated faster and has less time to undergo spontaneous decarboxylation to itaconic acid. The amorphous $Nb_2O_5.nH_2O$ however starts to crystallize at temperatures above 200 °C, which implies a loss of structure defects and acid sites.[35] Consequently, conventional high temperature reduction procedures with molecular hydrogen are not preferred. In this work, the reduction of Pd is therefore approached by a thermochemical reduction of palladium(II) acetate in propylene carbonate at 100 °C ($Pd/Nb_2O_5.nH_2O$ – PC) in order to maintain the amorphous nature of the $Nb_2O_5.nH_2O$ support.[36,37] Three catalysts with different metal loadings were synthesized, whereby the $Nb_2O_5.nH_2O$ was directly added to the propylene carbonate together with a certain amount of Pd(II) acetate, after which the resulting mixture was stirred and heated for 3 hours. For comparative reasons, also a wet impregnation synthesis method with $Pd(NH_3)_4(NO_3)_2$ was applied, whereby the reduction of Pd was performed in presence of molecular hydrogen at 300 °C ($Pd/Nb_2O_5.nH_2O$ – WI). Based on Pd ICP analysis, all the Pd was deposited onto the $Nb_2O_5.nH_2O$ for both methods.

The acidity of the supported catalysts was characterized by pyridine adsorption followed by FTIR spectroscopy. The estimated amounts of Brønsted and Lewis acid sites of the $Nb_2O_5.nH_2O$ and the bifunctional $Pd/Nb_2O_5.nH_2O$ catalysts are shown in Table 3. For the $Pd/Nb_2O_5.nH_2O$ – PC catalysts, the acid site densities of the $Nb_2O_5.nH_2O$ are well preserved, indicating that this synthesis method did not change the structural properties of the $Nb_2O_5.nH_2O$ support. Only the Brønsted acid density had a small drop at a higher loading of 1 wt%. For the 1 wt% $Pd/Nb_2O_5.nH_2O$ – WI catalyst, both the Brønsted and Lewis acid densities were significantly lower compared to the

$Nb_2O_5.nH_2O$ support and the 1 wt% $Pd/Nb_2O_5.nH_2O$ – PC catalyst. The reduction temperature of 300 °C thus clearly affected the structural properties of the amorphous $Nb_2O_5.nH_2O$. This is supported by the XRD diffractograms of both bifunctional catalysts (Figure S5), where $Pd/Nb_2O_5.nH_2O$ – PC is clearly amorphous, while some crystallinity is observed for the $Pd/Nb_2O_5.nH_2O$ – WI catalyst, with a small diffraction peak noted at 18.1°.

Table 3. Acid site densities of the synthesized bifunctional $Pd/Nb_2O_5.nH_2O$ catalysts estimated by pyridine-adsorption measurements with FTIR.

	Acid site density (µmol/g)	
Catalyst	Brønsted acid	Lewis acid
$Nb_2O_5.nH_2O$	206	251
0.2 wt% $Pd/Nb_2O_5.nH_2O$ - PC	194	261
0.6 wt% $Pd/Nb_2O_5.nH_2O$ - PC	190	258
1.0 wt% $Pd/Nb_2O_5.nH_2O$ - PC	149	257
1.0 wt% $Pd/Nb_2O_5.nH_2O$ - WI	94	135

Information on the dispersion, size and morphology of the Pd particles on the bifunctional catalysts was gathered by X-ray absorption spectroscopy (XAS), CO chemisorption and high angle annular dark field scanning transmission electron microscopy (HAADF-STEM) in combination with energy-dispersive X-ray spectroscopy (EDX). From the HAADF-STEM images, it was clear that for catalysts synthesized via the thermochemical reduction in propylene carbonate a homogeneous distribution of crystalline spherical Pd nanoparticles was obtained, supported on an amorphous $Nb_2O_5.nH_2O$ support (Figure 4, S7-S9 and S11). Pd particles on the $Pd/Nb_2O_5.nH_2O$ – WI catalyst, on the other hand, were found to be more heterogeneous and very large Pd particles up to 130 nm were observed on this catalyst (Figure 4, S10 and S12).

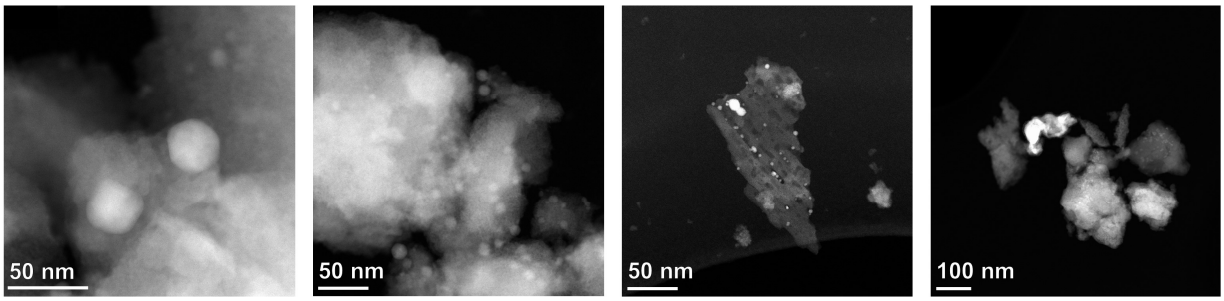

Figure 4. HAADF-STEM pictures of (left to right): 0.2 wt% Pd/Nb_2O_5.*n*H_2O – PC, 0.6 wt% Pd/Nb_2O_5.*n*H_2O – PC, 1.0 wt% Pd/Nb_2O_5.*n*H_2O – PC and 1.0 wt% Pd/Nb_2O_5.*n*H_2O – WI.

Next, the Pd dispersion and particle size of the bifunctional catalysts were also estimated by CO chemisorption and XAS, since these techniques render a more general image of these characteristics compared to the more local characterization by HAADF-STEM. Again, a clear difference is observed between both synthesis methods, where the Pd nanoparticles are significantly smaller when the thermochemical reduction with propylene carbonate is performed (Table S4 & Table S5). At low loadings of 0.2 wt% and 0.6 wt% for the Pd/Nb_2O_5.*n*H_2O – PC catalysts, a dispersion of 23% is achieved, while at 1.0 wt% the dispersion decreased to 13%. However, from the XANES spectra of the 0.6 wt% and 1.0 wt% Pd/Nb_2O_5.*n*H_2O – PC catalysts, it is observed that not all of the Pd(II) acetate is reduced during the thermochemical reduction (Figure 5a). An estimation of the Pd particle size from the X-ray absorption data is subsequently made based on the Pd-Pd coordination number, assuming that the nanoparticles possess a spherical shape (Figure 5b, Table S5). By leaving the contribution of the remaining Pd(II) oxide and Pd(II) acetate out from the calculations, the size of the total Pd particle is underestimated, since only the Pd^0 core is taken into account. As a result, the estimation of the Pd particle size by X-ray absorption techniques is smaller compared to the estimation by CO chemisorption analysis, which cannot distinguish these Pd^0 cores from the unreduced Pd(II) as clearly. In addition, prior to CO chemisorption, the catalyst is pre-treated at 200 °C under H_2 atmosphere, which might induce

further reduction of the Pd nanoparticles and thus result in a larger estimation of the particle sizes compared to the estimations obtained from the XAS data.

Further in-depth analysis of the XAS data also revealed another feature of the catalytic surface, namely the presence of Pd carbide bulk species in the Pd/Nb_2O_5.nH_2O catalysts, which is evidenced by both an increase in absorption in the immediate region after the Pd L_3-edge (Figure 5a, around 24370 eV) and an increased Pd-Pd distance (Figure 5b).[38,39] The origin of this Pd carbide phase might be the decomposition of a little propylene carbonate during the thermochemical reduction, forming some carbonaceous material which will then be incorporated into the Pd lattice.[40]

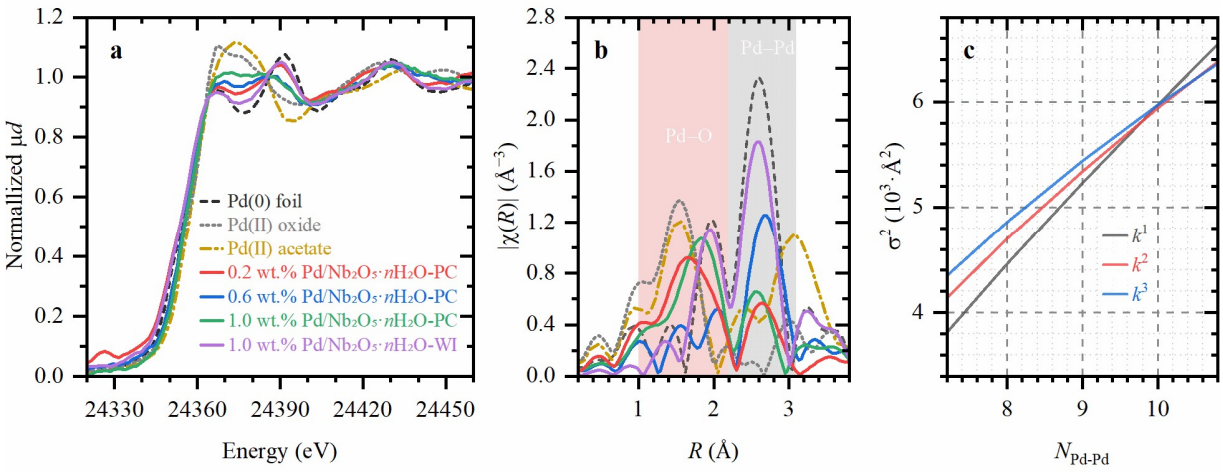

Figure 5. XANES (a) and FT-EXAFS (b) spectra of reference Pd(0) foil (dashed black), Pd(II) oxide (dotted grey) and Pd(II) acetate (dash-dot orange) and bifunctional Pd/Nb_2O_5.nH_2O - PC catalysts (solid lines). Part (c) demonstrates the procedure applied to overcome the correlations between Debye-Waller parameter and coordination number.

2.4. Bifunctional Pd/Nb_2O_5.nH_2O catalysts – Catalytic performance & Substrate scope

The bifunctional materials were used as catalysts for the sequential dehydration-hydrogenation of citric acid to PTA, and compared to the two-catalyst one-pot system (Table 4). To make correct comparisons, the same amount of Nb_2O_5.nH_2O was used in each batch reaction. 1.0 mol% of Pd

in the two-catalyst one-pot system represents the same loading of Pd as 0.2 wt% of Pd on a $Nb_2O_5.nH_2O$ support. Regarding both reduction methods, the results demonstrate that the bifunctional $Pd/Nb_2O_5.nH_2O$ obtained *via* a wet impregnation method (entry 1) performs worse in comparison to the one that is obtained *via* a thermochemical reduction in propylene carbonate (entry 2), since both the conversion of citric acid and the selectivity towards PTA are significantly lower. The decrease in citric acid conversion for the $Pd/Nb_2O_5.nH_2O$ – WI catalyst can be attributed to the lower density of acid sites (Table 3), while the lower selectivity towards PTA can be associated with the significantly larger Pd particles and lower Pd dispersion (Figure 4, Table S4 & Table S5). In presence of the $Pd/Nb_2O_5.nH_2O$ – PC catalysts, high selectivities towards PTA are observed for all loadings (entry 2 – 4); these are at least as high as the selectivity obtained with the two-catalyst one-pot system (entry 5). Thus, a close intimacy between the acid and hydrogenation catalytic sites allows to reach the desired high selectivities for PTA, even at low Pd loadings of 0.2 wt%. Even though the XAS data showed the presence of a Pd carbide bulk phase and demonstrated that not all of the Pd(II) was reduced, this does not seem to hamper the catalytic activity of the $Pd/Nb_2O_5.nH_2O$ – PC catalysts. However, lower conversions were observed in the case of the bifunctional catalysts. One reason might be that the acid sites of the $Pd/Nb_2O_5.nH_2O$ catalysts are hindered by some residual propylene carbonate or acetic acid, since those organics were clearly detected in the ^{1}H-NMR spectra of the reaction mixtures. Consequently, it can be expected that for the catalysts with higher Pd loadings more acetic acid will be present on the catalytic surface initially, which translates in a slower conversion of citric acid as well as a lower mole balance, since a large fraction of the adsorbed citric acid is still not converted after 20 h. This would translate into an overestimation of the amount of acetic acid that is produced from citric acid in the catalytic reaction in presence of $Pd/Nb_2O_5.nH_2O$ – PC catalysts, and thus in a slight

overestimation of the selectivity towards fragmented products in Table 4 (entry 2 – 4). Higher loadings of Pd however do decrease the selectivity towards MSA, indicating that aconitic acid is hydrogenated faster if more Pd nanoparticles are present on the $Nb_2O_5.nH_2O$ surface.

The reusability of the two best performing Pd/$Nb_2O_5.nH_2O$ – PC catalysts (0.2 wt% and 0.6 wt%) was examined. Figure 6 shows the mole balance, product distribution and remaining fraction of citric acid during the recycle runs, along with the cumulative amount of Pd that is leached after five runs. Regarding the latter, it can be concluded that these catalysts remain stable under the aqueous acidic reaction conditions since only a very small amount of Pd was leached. Remarkably, these catalysts seem to become more active as the number of runs adds up, as indicated by the increase in citric acid conversion (Table S6) and hydrogenated product yields (Figure 6). Whereas the increase of conversion and mole balance from the 1st to the 2nd run can be attributed to the replacement of residual adsorbed molecules on the surface (*vide supra*) by citric acid, this does not fully explain the further increase in conversion upon subsequent recycle runs, since the surface will be loaded with citric acid after the first cycle. A possible explanation for this unexpected phenomenon is that the surface of the $Nb_2O_5.nH_2O$ support, and thus also the associated Brønsted/Lewis acid ratio, is somewhat influenced and changed by the continued exposure to a citric acid solution at elevated temperatures, with even an improved activity as a consequence. Comparing both catalysts, overall higher conversions are obtained in presence of the 0.6 wt% Pd/$Nb_2O_5.nH_2O$ – PC catalyst. Since the acidity of both catalysts is nearly identical (Table 3), the higher conversion of citric acid is presumably a result of the higher Pd loading; the presence of a larger amount of well-dispersed Pd nanoparticles will lead to a faster encounter of the intermediate aconitic acid with a hydrogenation site and will leave less time for aconitic acid to hydrate again to citric acid. A higher loading, however, does not further increase the selectivity towards PTA,

since the latter reached comparable high values (92% - 96%) during all recycling runs of both catalysts (Table S6). This consistently high selectivity towards PTA makes the bifunctional catalysts clearly stand out compared to the two-catalyst one-pot system, since for this system a significant drop in selectivity to PTA was observed upon recycling (Table 1, entry 6) or upon presaturation (Figure 1, Profile F). This also confirms once more the stability of the $Pd/Nb_2O_5.nH_2O$ – PC catalysts. To conclude, yields up to 91% of PTA were achieved during these recycling runs.

Table 4. Sequential dehydration-hydrogenation of citric acid in presence of bifunctional $Pd/Nb_2O_5.nH_2O$ catalysts. [a]

				Selectivity [%]			
Entry	Catalyst(s)	Amount Pd	X [%][b]	PTA[c]	MSA[d]	Fragmentation[e]	Mole balance [%]
1	$Pd/Nb_2O_5.nH_2O$ - WI	1.0 wt% [g]	62	86	12	2	88
2	$Pd/Nb_2O_5.nH_2O$ - PC	1.0 wt% [g]	71	93	2	5	71
3	$Pd/Nb_2O_5.nH_2O$ - PC	0.6 wt% [g]	77	94	3	3	77
4	$Pd/Nb_2O_5.nH_2O$ - PC	0.2 wt% [g]	76	93	5	2	82
5	$Nb_2O_5.nH_2O$ + Pd/C	1.0 mol% [f]	86	91	8	1	86

[a] Reaction conditions: Citric acid (0.2 mmol) in water (2 mL), 0.1 g of $Nb_2O_5.nH_2O$ or $Pd/Nb_2O_5.nH_2O$, 10 bar H_2, 160 °C, 20 h. [b] Conversion: sum of the amount of detected products in the reaction mixture divided by the initial amount of citric acid that was added. Potentially adsorbed species are not taken into account; these consist solely of citric acid. [d] Methylsuccinic acid. [e] 'Fragmentation' represents acetone and acetic acid. [f] mol% of Pd (5 wt% Pd/C) with respect to citric acid. [g] wt% of Pd with respect $Nb_2O_5.nH_2O$ where 0.2 wt% equals 1 mol%. The wt% of Pd was verified by Pd-ICP.

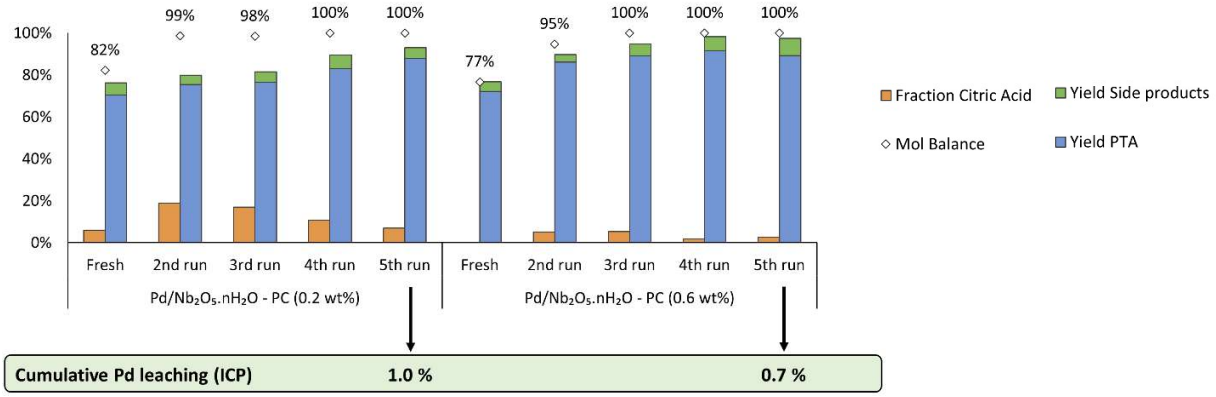

Figure 6. Direct reuse of the catalytic system with $Pd/Nb_2O_5.nH_2O$ catalysts. The cumulative Pd leaching, determined by ICP and noted as a percentage of the initial Pd loading, is denoted at the bottom. Reaction conditions: 0.1 g $Pd/Nb_2O_5.nH_2O$, citric acid 0.2 mmol, water 2 mL, 10 bar H_2, 160 °C, 20 h. For subsequent

runs, the amount of citric acid and volume of water were adjusted if some loss of catalyst was observed. Legend: Citric acid (orange), PTA (blue), side products* (green) and mole balance (white diamond & denoted on top in percentage). * Side products consist of MSA and fragmented products such as acetic acid or acetone.

Finally, a small substrate scope investigation was performed on different hydroxy-carboxylic acids to illustrate the potential of the bifunctional dehydration-hydrogenation with Pd/Nb_2O_5.*n*H_2O – PC catalysts (Table 5). Very selective formation of the saturated (di)carboxylic acid was obtained in case of malic acid (entry 2) and β-hydroxybutyric acid (entry 3); however the temperature had to be increased slightly to obtain high yields. Even γ-valerolactone (GVL) could be converted very selectively to valeric acid in presence of Pd/Nb_2O_5.*n*H_2O catalysts. Although a temperature of 200 °C was required to obtain a respectable conversion of GVL, this temperature is still mild in comparison to previously reported Brønsted acid catalysed ring-opening hydrogenation of GVL to valeric acid.[41-43] This illustrates once again that the Nb_2O_5.*n*H_2O support retains its strong Brønsted acidic properties, even under aqueous conditions. When the dihydroxy sugar acid tartaric acid was applied as a substrate, mainly lactic acid was observed (entry 4) and in a smaller fraction the desired product succinic acid. To obtain succinic acid from tartaric acid, a twofold sequential dehydration-hydrogenation has to be performed. However, the large fraction of lactic acid in the product mixture, indicates that mainly a different route is struck. After the first dehydration of tartaric acid, enol-oxaloacetic acid is obtained, which will tautomerize to oxaloacetic acid (Figure S13). This oxaloacetic acid intermediate is known to decarboxylate spontaneously to pyruvic acid, which might be expected to be a stable end product.[44,45] However, under the applied aqueous acidic conditions, pyruvic acid will be in equilibrium with its geminal diol 2,2-dihydroxypropane diol and might thus be susceptible to a sequential dehydration-hydrogenation to obtain lactic acid as the final end product.[46] Further dehydration of lactic acid

to acrylic acid and subsequent hydrogenation to propionic acid were not observed. From this substrate investigation, it becomes clear that the bifunctional Pd/Nb_2O_5.*n*H_2O – PC catalysts of this work are efficient to remove a hydroxyl group of (biobased) monohydroxy carboxylic acids *via* a green and mild dehydration-hydrogenation process, even if the hydroxyl group is present as a lactone function. However, to expand the substrate group to di- and polyhydroxylated carboxylic acids for the production of saturated diacids, further research has to be conducted.

Table 5. Substrate scope investigation with 0.6 wt% Pd/Nb_2O_5.nH_2O [a]

Entry	Substrate	T [°C]	X [%][b]	Major product	S [%][c]	Minor product	S [%][c]
1	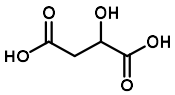	160	69	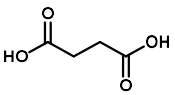	> 99	/	/
		170	88		> 99		
2	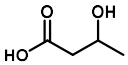	160	55	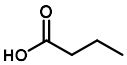	> 99	/	/
		175	93		> 99		
3	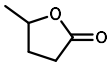	160	3	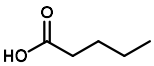	> 99	/	/
		200	50		> 99		
4[d]	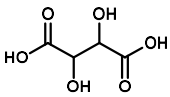	160*	> 99	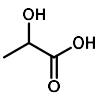	77	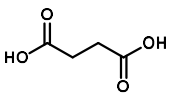	11
		180*	> 99		63		16

[a] Reaction conditions: 0.2 mmol substrate in 2 mL water, 0.1 g 0.6 wt% Pd/Nb_2O_5.nH_2O, 10 bar H_2, 20 h. [b] Conversion: calculated based on the amount of detected products in the reaction mixture divided by the initial amount of substrate. Potentially adsorbed compounds are not taken into account. [c] Selectivity. [d] Conversion of tartaric acid was determined by HPLC (ESI). * 30 bar H_2.

3. CONCLUSIONS

Tricarballylic acid, an interesting plasticizer precursor, can be obtained directly from citric acid *via* a new sequential dehydration-hydrogenation reaction pathway. In this work, Nb_2O_5.nH_2O was found to be an active solid acid dehydration catalyst that remained stable in the corrosive citric acid reaction mixture. The interaction between citric acid and the Nb_2O_5.nH_2O catalyst was investigated by ^{13}C MAS NMR spectroscopy, where an unequivocal interaction of the hydroxyl group of citric acid with the Nb_2O_5.nH_2O surface was observed. In a second stage, bifunctional

$Pd/Nb_2O_5.nH_2O$ catalysts were synthesized *via* a low temperature thermochemical reduction method in propylene carbonate. By this approach, not only well-dispersed Pd-nanoparticles were obtained, but also the acid site density of the $Nb_2O_5.nH_2O$ support remained preserved, which is key to maintain an efficient dehydration-hydrogenation process. By bringing the acid and hydrogenation sites close to one another, the aconitic acid intermediate will be hydrogenated fast, leading to high tricarballylic acid selectivities up to 94%. A substrate scope investigation ensured the potential of these $Pd/Nb_2O_5.nH_2O$ catalysts for the sequential dehydration-hydrogenation of other monohydroxy (biobased) carboxylic acids. In conclusion, we have developed a catalytic dehydration-hydrogenation system that is green, active under aqueous conditions, highly selective, recyclable and operates under relatively mild reaction conditions.

AUTHOR INFORMATION

Corresponding Author

Dirk E. De Vos - *Centre for Membrane Separations, Adsorption, Catalysis and Spectroscopy for Sustainable Solutions (cMACS), Department of Molecular Systems (M^2S), KU Leuven, 3001 Leuven, Belgium;* orcid.org/0000-0003-0490-9652; Email: dirk.devos@kuleuven.be

Authors

Wouter Stuyck - *Centre for Membrane Separations, Adsorption, Catalysis and Spectroscopy for Sustainable Solutions (cMACS), Department of Molecular Systems (M^2S), KU Leuven, 3001 Leuven, Belgium;* orcid.org/0000-0002-2887-0580

Aram L. Bugaev – *The Smart Materials Research Institute, Southern Federal University, 344090 Rostov-on-Don, Russia;* orcid.org/0000-0001-8273-2560

Tom Nelis – *Centre for Membrane Separations, Adsorption, Catalysis and Spectroscopy for Sustainable Solutions (cMACS), Department of Molecular Systems (M^2S), KU Leuven, 3001 Leuven, Belgium;* https://orcid.org/0000-0003-3797-408X

Rodrigo de Oliveira-Silva – *Centre for Membrane Separations, Adsorption, Catalysis and Spectroscopy for Sustainable Solutions (cMACS), Department of Molecular Systems (M^2S), KU Leuven, 3001 Leuven, Belgium;* orcid.org/0000-0003-3903-2678

Simon Smolders – *Centre for Membrane Separations, Adsorption, Catalysis and Spectroscopy for Sustainable Solutions (cMACS), Department of Molecular Systems (M^2S), KU Leuven, 3001 Leuven, Belgium;* orcid.org/0000-0002-3622-2022

Oleg A. Usoltsev – *The Smart Materials Research Institute, Southern Federal University, 344090 Rostov-on-Don, Russia;* orcid.org/0000-0002-1537-3497

Daniel Arenas Esteban - *Electron Microscopy for Materials Science (EMAT), University of Antwerp, Groenenborgerlaan 171, 2020 Antwerpen, Belgium*; orcid.org/0000-0002-5626-9848

Sara Bals - *Electron Microscopy for Materials Science (EMAT), University of Antwerp, Groenenborgerlaan 171, 2020 Antwerpen, Belgium*; orcid.org/0000-0002-4249-8017

Dimitrios Sakellariou – *Centre for Membrane Separations, Adsorption, Catalysis and Spectroscopy for Sustainable Solutions (cMACS), Department of Molecular Systems (M^2S), KU Leuven, 3001 Leuven, Belgium;* orcid.org/0000-0001-7424-5543

DECLARATION OF INTEREST STATEMENT

The authors declare that they have no known competing financial interests or personal relationships that could have appeared to influence the work reported in this paper.

ACKNOWLEDGMENTS

W.S. is grateful to the FWO for his SB PhD fellowship (1SC1519N). D. E. D. V. acknowledges KU Leuven for long-term structural funding through Metusalem program Casas (METU14/04). D.E.D.V. thanks FWO for project support (G0D0518N and G0F2320N). S.B. and D.A.E. are grateful to the European Research Council (ERC-CoG-2019 815128). A.L.B. and U.O.A. acknowledges the President's Grant of Russian Federation MK-5853.2021.1.2 for funding (XAS investigation). Synchrotron experiments were supported by the Russian Science Foundation (grant #20-43-01015; joint RSF-FWO project).

ABBREVIATIONS

MAS NMR, magic angle spinning nuclear magnetic resonance; XAS, x-ray absorption spectroscopy; ATBC, acetyl tributyl citrate; BTHC, butyryl trihexyl citrate; DEHP, bis(2-ethylhexyl) phthalate; PVC, polyvinyl chloride; PTA, propane-1,2,3-tricarboxylic acid; ICP, inductively coupled plasma; ppb, parts per billion; MSA, methylsuccinic acid; ATR-FTIR, attenuated total reflection-Fourier transform infrared; PC, propylene carbonate; WI, Wet impregnation; XANES, x-ray absorption near edge spectroscopy; GVL, γ-valerolactone.

REFERENCES

[1] Groh, K. J.; Backhaus, T.; Carney-Almroth, B.; Geueke, B.; Inostroza, P. A.; Lennquist, A.; Leslie, H. A.; Maffine, M.; Slunge, D.; Trasande, L.; Warhurst, A. M.; Muncke J. Overview of known plastic packaging-associated chemicals and their hazards. *Science of The Total Environment* **2019**, *651*, 3253-3268, https://doi.org/10.1016/j.scitotenv.2018.10.015

[2] Walters, P.; Cadogan, D. F.; Howick, C. J. Plasticizers. In *Ullmann's Encyclopedia of Industrial Chemistry*; Wiley-VCH Verlag GmbH & Co: Weinheim, Germany, 2020; pp. 1-27.

[3] Bocqué, M.; Voirin, C.; Lapinte, V.; Caillol, S.; Robin, J.-J. Petro-based and bio-based plasiticizers: Chemical structures to plasticizing properties. *Journal of Polymer Science, Part A: Polymer Chemistry* **2016**, *54*, 11-33, https://doi.org/10.1002/pola.27917

[4] Bueno-Ferrer, C.; Garrigós, M. C.; Jiménez, A. Characterization and thermal stability of poly(vinyl chloride) plasticized with epoxidized soybean oil for food packaging. *Polym. Degrad. Stab.* **2010**, *95*, 2207-2212, https://doi.org/10.1016/j.polymdegradstab.2010.01.027

[5] Yin, B.; Hakkarainen, M. Oligomeric isosorbide esters as alternative renewable resource plasticizers for PVC. *J. Appl. Polym. Sci.* **2011**, *119*, 2400-2407, https://doi.org/10.1002/app.32913

[6] Greco, A.; Brunetti, D.; Renna, G.; Mele, G.; Maffezzoli, A. Plasticizers for poly(vinyl chloride) from cardanol as a renewable resource. *Polym. Degrad. Stab.* **2010**, *95*, 2169-2174, https://doi.org/10.1016/j.polymdegradstab.2010.06.001

[7] Yu, Z.; Zhou, J.; Zhang, J.; Huang, K.; Cao, F.; Wei, P. Evaluating effects of biobased 2,5-furanedicarboxylate esters as plasticizers on the thermal and mechanical properties of poly(vinyl chloride). *J. Appl. Polym. Sci.* **2014**, *131*, 40938-40948, https://doi.org/10.1002/app.40938

[8] Matos, M.; Cordeiro, R. A.; Faneca, H.; Coelho, J. F. J.; Silvestre, A. J. D.; Sousa, A. E. Replacing Di(2-ethylhexyl) Terephthalate by Di(2-ethylhexyl) 2,5-Furandicarboxylate for PVC Plasticization: Synthesis, Materials Preparation and Characterization. *Materials* **2019**, *12*, 2336-2351, https://doi.org/10.3390/ma12142336

[9] Chiellinni, F.; Ferri, M.; Morelli, A.; Dipaola, L.; Latini, G. Perspectives on alternatives to phthalate plasticized poly(vinyl chloride) in medical devices applications. *Progress in Polymer Science* **2013**, *38*, 1067-1088, https://doi.org/10.1016/j.progpolymsci.2013.03.001

[10] Sweis, I. E.; Cressey, B. C. Potential role of the common food additive manufactured citric acid in eliciting significant inflammatory reactions contributing to serious disease states: A series of four case reports. *Toxicol. Rep.* **2018**, *5*, 808-812, https://doi.org/10.1016/j.toxrep.2018.08.002

[11] Fisk, J. M.; Pisciotto, P. T., Snyder, E. L.; Perrotta, P. L. Platelets and Related Products. In *Blood banking and transfusion medicine 2nd ed.*; Elsevier: Churchill Livingstone, Philadelphia, United States of America, 2007; pp. 308-341.

[12] *Acetylation*: *a)* Chao-Hung, H.; Chun-Ho, X.; Wei-Guang, J. Catalytic synthesizing method of acetyl tri-in-butyl citrate. CN1303055C, 2007. *b)* Ting, S. Synthetic method of high-purity acetyl tributyl citrate (ATBC). CN101353305B, 2007. *c)* Bing, L.; Guanxun, S.; Zuli, Z.; Zhen, Y.; Yanli, W.; Junyun, W. Process for producing acet-tributyl citrate. CN101402571A, 2008. *d*) Kai, G.; Yang, Z.; Pengwei, Z.; Wei, H.; Xiaolin, L. Technology for synthesizing acetyl

citrate. CN102351696B, 2011. *e)* Jianzhong, L.; Yibeng, Z.; Huilai, L. Integrated production technique of acetyl tributyl citrate (ATBC). CN102633640B, 2012. *f)* Xingjian, C. A kind of high-efficiency synthesis method of tributyl 2-acetylcitrate. CN106928065A, 2017. *Butyrylation: a)* Day, J. F. Acylated esters. U. S. Patent US20060094894A1, 2004.

[13] Welle, F.; Wolz, G.; Franz, R. Migration of plasticizers from PVC tubes into enteral feeding solutions. *Pharma International* **2005**, *3*, 17-21.

[14] SCENIHR, Preliminary report on the safety of medical devices containing DEHP-plasticized PVC or other plasticizers on neonates and other groups possibly at risk. 2007.

[15] Reid, R. J.; Fulton, C.; Smith Jr., W. M.; Falls, C.; Werner, B. H. Plasticization of vinylidene resins with tricarballylates. U. S. Patent US2802802, 1957.

[16] Magne, F. C.; Mod, R. R. Plasticizers from Aconitic and Tricarballylic Acids. *Ind. Eng. Chem.* **1953**, *45*, 1546-1547, https://doi.org/10.1021/ie50523a049

[17] Stuyck, W.; Verduyckt, J.; Krajnc, A.; Mali, G.; De Vos, D. E. Selective defunctionalization of citric acid to tricarballylic acid as a precursor for the production of high-value plasticizers. *Green Chem.* **2020**, *22*, 7812-7822, https://doi.org/10.1039/D0GC02298E

[18] Nakajima, K.; Hirata, J.; Kim, M.; Gupta, N. K.; Murayama, T.; Yoshida, A.; Hiyoshi, N.; Fukuoka, A.; Ueda, W. Facile Formation of Lactic Acid from a Triose Sugar in Water over Niobium Oxide with a Deformed Orthorhombic Phase. *ACS Catalysis* **2018**, *8*, 283-290, https://doi.org/10.1021/acscatal.7b03003

[19] Xu, S.; Shen, S.; Xiong, W.; Zhao, S.; Zuo, L.; Wang, L.; Zeng, W.; Chu, S.; Chen, P.; Lin, Y.; Qian, K.; Huang, W.; Liang, H. High-Temperature Synthesis of Small-Sized Pt/Nb Alloy Catalysts on Carbon Supports for Hydrothermal Reactions. *Inorg. Chem.* **2020**, *59*, 15953-15961, https://doi.org/10.1021/acs.inorgchem.0c02457

[20] Tanabe, K. Niobic acid as an unusual acidic solid material. *Materials Chemistry and Physics* **1987**, *17*, 217-225, https://doi.org/10.1016/0254-0584(87)90057-5

[21] Tanabe, K.; Okazaki, S. Various reactions catalyzed by niobium compounds and materials. *Applied Catalysis A: General* **1995**, *133*, 191-218, https://doi.org/10.1016/0926-860X(95)00205-7

[22] Nowak, I.; Ziolek, M. Niobium Compounds: Preparation, Characterization, and Application in Heterogeneous Catalysis. *Chem. Rev.* **1999**, *99*, 3603-3624, https://doi.org/10.1021/cr9800208

[23] Tanabe, K. Catalytic application of niobium compounds. *Catalysis Today* **2003**, *78*, 65-77, https://doi.org/10.1016/S0920-5861(02)00343-7

[24] Nakajima, K.; Baba, Y.; Noma, R.; Kitano, M.; Kondo, J. N.; Hayashi, S.; Hara, M. $Nb_2O_5.nH_2O$ as a Heterogeneous Catalyst with Water-Tolerant Lewis Acid Sites. *J. Am. Chem. Soc.* **2011**, *133*, 4224-4227, https://doi.org/10.1021/ja110482r

[25] Verduyckt, J.; De Vos, D. E. Highly selective one-step dehydration, decarboxylation and hydrogenation of citric acid to methylsuccinic acid. *Chem. Sci.* **2017**, *8*, 2616-2620, https://doi.org/10.1039/C6SC04541C

[26] Verduyckt, J.; Geers, A.; Claes, B.; Eyley, S.; Van Goethem, C.; Stassen, I.; Smolders, S.; Ameloot, R.; Vankelecom, I.; Thielemans, W.; De Vos, D. E. Stabilising Ni catalysts for the dehydration-decarboxylation-hydrogenation of citric acid to methylsuccinic acid. *Green Chem.* **2017**, *19*, 4642-4650, https://doi.org/10.1039/C7GC01773A

[27] Le Nôtre, J.; Witte-van Dijk, S. C. M.; van Haveren, J.; Scott, E. L.; Sanders, J. P. M. Synthesis of Bio-Based Methacrylic Acid by Decarboxylation of Itaconic Acid and Citric Acid Catalyzed by Solid Transition-Metal Catalysts. *ChemSusChem*, **2014**, *7*, 2712-2720, https://doi.org/10.1002/cssc.201402117

[28] Omata, K.; Nambu, T. Catalysis of water molecules acting as Brönsted acids at Lewis acid sites on niobium oxide. *Applied Catalysis A: General* **2020**, *607*, 117812, https://doi.org/10.1016/j.apcata.2020.117812

[29] Martin, R. B. Citrate Binding of Al^{3+} and Fe^{3+}. *Journal of Inorganic Biochemistry* **1986**, *28*, 181-187, https://doi.org/10.1016/0162-0134(86)80081-2

[30] Lindegren, M.; Loring, J. S.; Persson, P. Molecular Structures of Citrate and Tricarballylate Adsorbed on α-FeOOH Particles in Aqueous Suspensions. *Langmuir* **2009**, *25 (18)*, 10639-10647, https://doi.org/10.1021/la900852p

[31] Mudunkotuwa, I. A.; Grassian, V. H. Citric Acid Adsorption on TiO_2 Nanoparticles in Aqueous Suspensions at Acidic and Circumneutral pH: Surface Coverage, Surface Speciation, and Its Impact on Nanoparticle-Nanoparticle Interactions. *J. Am. Chem. Soc.* **2010**, *132*, 14986-14994, https://doi.org/10.1021/ja106091q

[32] Zhang, X.; Chen, L.; Liu, R.; Li, D.; Ge, X.; Ge, G. The Role of the OH Group in Citric Acid in the Coordination with Fe_3O_4 Nanoparticles. *Langmuir* **2019**, *35 (25)*, 8325-8332, https://doi.org/10.1021/acs.langmuir.9b00208

[33] Hidber, P. C.; Graule, T. J.; Gauckler, L. J. Citric Acid – A Dispersant for Aqueous Alumina Suspensions. *J. Am. Ceram. Soc.* **1996**, *79 (7)*, 1857-1867, https://doi.org/10.1111/j.1151-2916.1996.tb08006.x

[34] Tamain, C.; Bonato, L.; Aupiais, J.; Dumas, T.; Guillaumont, D.; Barkleit, A.; Berthon, C.; Solari, P. L.; Ikeda-Ohno, A.; Guilbaud, P.; Moisy, P. Role of the Hydroxo Group in the Coordination of Citric Acid to Trivalent Americium. *Eur. J. Inorg. Chem.* **2020**, 1331-1334, https://doi.org/10.1002/ejic.202000124

[35] Yan, L.; Rui, X.; Chen, G.; Xu, W.; Zou, G.; Luo, H. Recent advances in nanostructured Nb-based oxides for electrochemical energy storage. *Nanoscale* **2016**, *8*, 8443-8465, https://doi.org/10.1039/C6NR01340F

[36] Reetz, M. T.; Lohmer, G. Propylene carbonate stabilized nanostructured palladium clusters as catalysts in Heck reactions. *Chem. Comm.* **1996**, 1921-1922, https://doi.org/10.1039/CC9960001921

[37] Demel, J.; Cejka, J.; Bakardjieva, S.; Stepnicka, P. Grafting of palladium nanoparticles onto mesoporous molecular sieve MCM-41: Heterogeneous catalyst for the formation of an *N*-substituted pyrrol. *Journal of Molecular Catalysis A: Chemical* **2007**, *263*, 259-265, https://doi.org/10.1016/j.molcata.2006.08.094

[38] Bugaev, A. L.; Guda, A. A.; Lazzarini, A. Lomachenko, K. A.; Groppo, E.; Pellegrini, R.; Piovano, A.; Emerich, H.; Soldatov, A. V., Bugaev, L. A.; Dmitriev, V. P.; van Bokhoven, J. A.; Lamberti, C. In situ formation of hydrides and carbides in palladium catalyst: When XANES is better than EXAFS and XRD. *Catalysis Today*, **2017**, *283*, 119-126, https://doi.org/10.1016/j.cattod.2016.02.065

[39] Bugaev, A. L.; Usoltsev, O. A.; Guda, A. A.; Lomachenko, K. A.; Pankin, I. A.; Rusalev, Y. V.; Emerich, H.; Groppo, E.; Pellegrini, R.; Soldatov, A. V.; van Bokhoven, J. A.; Lamberti, C. Palladium Carbide and Hydride Formation in the Bulk and at the Surface of Palladium Nanoparticles. *J. Phys. Chem. C* **2018**, *122*, 12029-12037, https://doi.org/10.1021/acs.jpcc.7b11473

[40] Tew, M. W.; Nachtegaal, M.; Janousch, M.; Huthwelker, T.; van Bokhoven, J. A. The irreversible formation of palladium carbide during hydrogenation of 1-pentyne over silica-supported palladium nanoparticles: *in situ* Pd K and L_3 edge XAS. *Phys. Chem. Chem. Phys.* **2012**, *14*, 5761-5768, https://doi.org/10.1039/C2CP24068H

[41] Lange, J.-P.; Price, R.; Ayoub, P. M.; Louis, J.; Petrus, L.; Clarke, L.; Gosselink, H. Valeric Biofuels: A Platform of Cellulosic Transportation Fuels. **2010**, *49*, 4479-4483, https://doi.org/10.1002/anie.201000655

[42] Serrano-Ruiz, J. C.; Wang, D. Dumesic, J. A. Catalytic upgrading of levulinic acid to 5-nonanone. *Green Chem.* **2010**, *12*, 574-577, https://doi.org/10.1039/B923907C

[43] Al-Naji, M.; Van Aelst, J.; Liao, Y.; d'Halluin, M.; Tian, Z.; Wang, C.; Gläser, R.; Sels, B. F. Pentanoic acid from γ-valerolactone and formic acid using bifunctional catalysis. **2020**, *22*, 1171-1181, https://doi.org/10.1039/C9GC02627D

[44] Tsai, C. S. Spontaneous decarboxylation of oxaloacetic acid. *Canadian Journal of Chemistry* **1967**, *45*, 873-880, https://doi.org/10.1139/v67-145

[45] Logue, M. W.; Pollack, R. M.; Vitullo, V. P. The Nature of the Transition State for the Decarboxylation of *β*-Keto Acids. *J. Am. Chem. Soc.* **1975**, *22*, 6868-6869, https://doi.org/10.1021/ja00856a047

[46] Marón, M. K.; Takahashi, K.; Shoemaker, R. K.; Vaida, V. Hydration of pyruvic acid to its germinal-diol, 2,2-dihydroxypropanoic acid, in a water-restricted environment. *Chem. Phys. Lett.*, **2011**, *513*, 184-190, https://doi.org/10.1016/j.cplett.2011.07.090